CrossMark

ORIGINAL

Adsorption of *cis*-dichlorodiammineplatinum by nanostructures based on single-domain magnetite

A. L. Petranovska[1] · N. V. Abramov[1] · S. P. Turanska[1] · P. P. Gorbyk[1] ·
A. N. Kaminskiy[2] · N. V. Kusyak[2]

Abstract Magnetosensitive nanocomposites on the basis of monodomain magnetite Fe_3O_4/*meso*-2,3-dimercaptosuccinic acid, Fe_3O_4/γ-aminopropyltriethoxysilane, Fe_3O_4/polyacrylamide, Fe_3O_4/hydroxyapatite were synthesized. Size distribution of magnetite nanoparticles in ensemble and their magnetic properties were studied. It has been shown that the magnetization curve of the liquid containing monodomain magnetite has a form that is characteristic for superparamagnetics, and its calculations in the framework of Langeven's paramagnetism theory match satisfactorily to the experimental results. The highest adsorption parameters were observed for magnetosensitive nanocomposites Fe_3O_4/polyacrylamide and Fe_3O_4/γ-aminopropyltriethoxysilane. Prospects of the studied nanostructures for medicobiological and technical applications as adsorbents of *cis*-dichlorodiammineplatinum were shown.

Keywords Adsorption · *cis*-dichlorodiammineplatinum · Magnetite · Nanocomposites · Surface · Adsorbents

Introduction

Use of adsorbents with magnetic properties considerably facilitates a problem of separation and gathering of substances and microbiological objects by the adsorption method [1–3]. Chemical modification and surface functionalization of adsorbents allow one to use them in various physical, chemical, and biological conditions, as well as to operate selectivity [4–10]. However, the available literature data let us conclude that elaboration of efficient adsorbents for ions and complexes of noble metals, in particular platinum, remains an actual problem [11, 12]. Platinum belongs to the most precious metals; therefore, its concentration and collection from technological wastage are economically favorable.

One of the directions to use platinum compounds, for example, on a basis of *cis*-dichlorodiammineplatinum, is production of medical preparations with cytostatic action applied in many schemes of modern cancer therapy. Application of the said preparations results in acute toxico-allergic reactions of an organism [13, 14]. Therefore, finding the ways for adsorptive detoxification of an organism in cancer therapy is especially promising. On the other hand, the problem of platinum utilization from the medicinal preparations that have lost suitability represents practical interest as well [15]. Such application is possible when magnetic nanoparticles are in the fluid environment. Therefore, clarification of behavior features of one-domain magnetite in composition of magnetic liquid is of interest.

One-domain magnetite was chosen as a starting material for synthesis of nanocomposites because of its unique physical and chemical properties, suitable biocompatibility and biodegradability, the gained experience in area of surface modification, opportunities for control of

✉ A. N. Kaminskiy
alexkamin@ukr.net

P. P. Gorbyk
pgorbyk@mail.ru; gorbyk@isc.gov.ua

[1] Chuiko Institute of Surface Chemistry, National Academy of Sciences of Ukraine, 17 General Naumov Str., Kiev 03164, Ukraine

[2] Ivan Franko Zhytomyr State University, 40 V. Berdychevska Str., Zhytomyr 10008, Ukraine

🦋 ⚘ Springer

movement of nanoparticles in liquid by means of an external magnetic field, application of magnetic separation method at stages of division, and extraction of adsorbents [4–6]. The monodomain condition of magnetic particles is characterized by uniformity of magnetization at any values and directions of field H, possibility of existence of domains not only in solid-state of ferro- and ferrimagnetic alloys and compounds, but also in liquid media (suspensions and colloids). In many practically important cases, the functional application of nanoparticles (directional transport of medicinal preparations to target organs and cells, recognition and decontamination of viruses, adsorption [4, 5, 10, 16, 17]) is carried out in liquid media. Besides, liquid is the most preferable form of magnetosensitive medicinal preparations for introduction in an organism [10].

To modify the surface of magnetite nanoparticles and to synthesize the nanocomposites, we used the substances biocompatible with a living organism: *meso*-2,3-dimercaptosuccinic acid, γ-aminopropyltriethoxysilane, hydroxyapatite, and polyacrylamide [5, 10, 11, 15, 18, 19].

The aim of this work was to study the properties of nanosized monodomain magnetite (Fe_3O_4) as a part of magnetic liquid, the adsorption of *cis*-dichlorodiammineplatinum on a surface of Fe_3O_4, nanocomposites: Fe_3O_4/*meso*-2,3-dimercaptosuccinic acid (DMSA), Fe_3O_4/hydroxyapatite (HA), Fe_3O_4/γ-aminopropylsiloxane (γ-APS), Fe_3O_4/polyacrylamide (PAA), and to perform comparative analysis of the results obtained.

Experimental part

Synthesis of nanosized magnetite

Synthesis of magnetite [5] was carried out by co-precipitation of iron salts according to the reaction:

$$Fe^{2+} + 2Fe^{3+} + 8NH_4OH \rightarrow Fe_3O_4 + 4H_2O + 8NH_4^+.$$
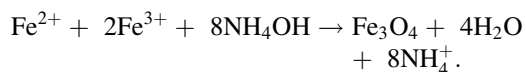
The prepared sol was precipitated applying the magnetic field and washed out by distilled water.

Particles of magnetite were characterized by the sizes of 3–23 nm and an ellipsoidal form as it was shown by methods of electron microscopy. Average particle size depends on synthesis conditions, size distribution could be operated technologically. The specific surface of the synthesized magnetite, depending on average particle size, was $S = 90$–180 m^2/g [as determined by nitrogen thermal desorption by means of KELVIN 1042 (COSTECH Instruments) device].

Modification of magnetite surface with *meso*-2,3-dimercaptosuccinic acid

Modification of magnetite nanoparticle surface with *meso*-2,3-dimercaptosuccinic acid [5] was performed by suspending magnetite particles (50 mg) in toluene (20 mL) with the same quantity of DMSA dissolved in 20 mL of dimethylsulfoxide. Reaction was carried out at ambient temperature during 24 h. The obtained reaction mixture was centrifuged; a sediment was washed with ethanol and distilled water, and dried up by air.

Modification of magnetite surface with γ-APTES

Modification of a surface of magnetite nanoparticles with γ-APTES was carried out by the liquid-phase method; in toluene [18, 19], γ-aminopropyltriethoxysilane (γ-APTES) was used as modifying agent. Oligomers were eliminated by distillation in vacuum. Before modification, magnetite was kept in 10 % solution of γ-APTES in toluene within 8 h for complete wetting of a surface.

Modification of magnetite surface with polyacrylamide

The process of magnetite surface modification with polyacrylamide [5] consisted in formation of a coating on the surface of nanosized magnetite by polymerization of acrylamide in high-frequency glow discharge plasma. As cross-linked agent, we used N,N'-methylene-bis-acrylamide. The analysis of kinetic curves of titration of double carbon–carbon bonds showed the complete polymerization of acrylamide layer within 2 min.

Modification of magnetite surface with hydroxyapatite

When modifying a surface of magnetite with hydroxyapatite, a necessary quantity of initial components was counted so that the molar ratio Ca:P was about 1.67:1.75 [5]. Hydroxyapatite cover on a surface of highly dispersive magnetite was prepared by sol–gel method according to the reaction:

$$10Ca(NO_3)_2 + 6(NH_4)_2HPO_4 + 8NH_3 + 2H_2O \rightarrow Ca_{10}(PO_4)_6(OH)_2 + 20NH_4NO_3.$$
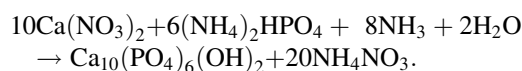
Using 15 % solution of NH_4OH, aqueous solutions containing 0.1 M $Ca(NO_3)_2 \cdot 4H_2O$ and 0.1 M $(NH_4)_2HPO_4$ were adjusted to pH = 11. The quantity of Fe_3O_4 was placed into $(NH_4)_2HPO_4$ solution, then $Ca(NO_3)_2$ solution was gradually added to it with intensive mixing. Reaction mixture was mixed within 1 h during heating at 100 °C and

left for 24 h. The formed Fe_3O_4/HA nanocomposite was washed out with distilled water until neutral pH and separated with permanent magnet. To obtain nanodispersed material, the reaction product was processed by ultrasound twice, with a break of 5–10 min, within 5 min.

Magnetic measurements

Hysteresis curves of magnetic moment of magnetite samples were measured at room temperature by means of vibration magnetometer at frequency of 228 Hz. For studies, we used the dry degaussed highly dispersive samples. To exclude interaction between particles, magnetite nanoparticles were placed in SiO_2 matrix. The installation and measurement technique is described in [21].

Biocompatibility research

Research on biocompatibility of magnetite was carried out by studying its influence on cell viability of baker's yeast *Saccharomyces cerevisiae*. Viability of cells was determined by a cytochemical method [20, 21].

Lower limit of magnetite cytotoxicity detection was observed at its concentration of 0.01 % (mass), and viability of cells was 98–99 %. At higher concentration of magnetite 0.05 % (mass), cellular agglomerates formed and viability of yeast decreased to $\sim$90 %.

Studies on adsorption of *cis*-dichlorodiammineplatinum complexes

Adsorption of *cis*-dichlorodiammineplatinum on a surface of nanosized magnetite and nanocomposites on their basis was carried out from solutions of *cis*-dichlorodiammineplatinum in physiological liquid. Calculations of adsorption capacity of nanostructures and concentration of solutions were made according to the contents of Pt^{2+} ions.

Solutions of *cis*-dichlorodiammineplatinum were prepared in the range of concentrations of Pt^{2+} from 10 to 200 mg/L. 0.03 L of the prepared solution of *cis*-dichlorodiammineplatinum was added to 0.1 g of a sorbent. Adsorption was carried out in dynamic regime within 3 h, using shaker, at pH = 7.1 and room temperature.

Adsorption capacity of nanostructures was determined by measuring Pt^{2+} concentration in solutions before and after adsorption with application of the atomic absorption analysis using a spectrophotometer C −115 M in flame acetylene-air mixture. Measurements were carried out at the wavelength of 265.7 nm.

Capacity of adsorbent A (mg/g) was calculated by the formula: $A = (C_0 - C_f) \times V/m$, where C_0 and C_f are concentration of Pt^{2+} ions in initial solution and after the sorption (mg/L), V is a volume of solution (L), and m is a mass of a sorbent (g). On the basis of the experimental results, adsorption isotherms were obtained and the parameters characterizing adsorption according to the Langmuir equation were calculated.

Distribution coefficients E (L/g) of Pt^{2+} ions between a surface of nanostructures and solution and extraction extent R (%) were determined by the formulas: $E = A/C_f, R = [(C_0 - C_f/C_0)] \times 100$, respectively.

Results and discussion

Fe_3O_4 phase was identified by X-ray diffraction analysis (DRON-4-07 diffractometer). Morphology studies of the dried-up magnetite samples performed using scanning atomic and magnetic power microscopy (Solver PRO-M device) revealed their inclination to form the aggregates with size up to 500 nm. Contours of atomic power and magnetic power images of particles coincided, showing absence of non-magnetic phases.

Ensembles of magnetite particles were investigated by transmission electron microscopy (TEM, Transmission Electron Microscope JEOL 2010). The histogram of particle size distribution ($N = 217$) and the curve of log-normal distribution are presented in Fig. 1a.

According to TEM, a diameter of particles is $d_{min} = 2.9$ nm and $d_{max} = 22.9$ nm. The size of an interval (h) should not exceed the value determined by Sturges' formula [22]: $(d_{max} - d_{min})/(1 + 3.33 \lg N) = 2.28$ nm. At $h = 2$ nm, the area of the sizes $[d_{min} + h/2, d_{max} + h/2]$ was divided into 11 identical intervals (Fig. 1a). The theoretical interval frequency m_k of existence in the ensemble of particles with a size belonging to k interval and belonging its middle was calculated using formulas [24]:

$$m_k = Nhf(d_k) \tag{1}$$

$$f(d_k) = \frac{1}{d_k \sigma_{\ln d} \sqrt{2\pi}} e - [\ln d_k - M(\ln d)]^2 \big/ 2\sigma^2 \ln d, \tag{2}$$

where $M(\ln d) = 2.14$ and $\sigma_{\ln d} = 0.42$ are the mathematical expectation and standard deviation of logarithmic size, respectively.

In [25], it is shown that absolute monodomain condition of magnetite particles ($T = 300$ K) is fulfilled at $d < 50$ nm. Thus, the particles in ensemble with sizes of 3–23 nm are absolutely monodomain ones. The analysis of values of saturation magnetization (σ_s) of magnetite monodispersions with various diameters of particles according to literary data allowed to find out an empirical dependence for calculation of σ_s for a particle with diameter d (nm) in the range of 4–42 nm:
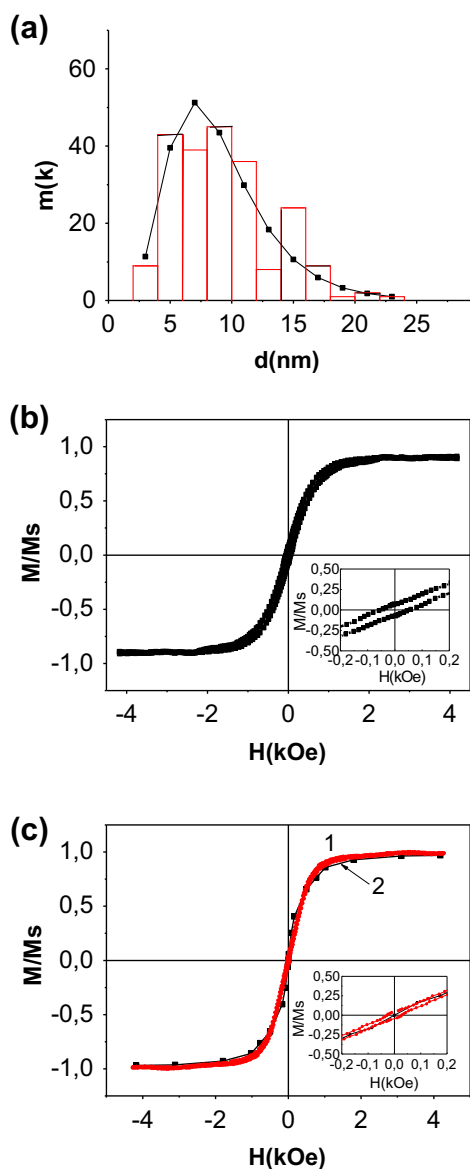
(a)

(b)

(c)

Fig. 1 Histogram of particle size distribution and curve of log-normal distribution with parameters: $M(d) = 9.38$ nm, $\sigma_d = 3.38$ nm (**a**). Magnetic hysteresis curves for ensemble of the modified nanoparticles Fe_3O_4/Na ol. (**b**) and magnetic liquid Fe_3O_4/Na ol. + H_2O (**c**) [experimental (*1*) and calculated (*2*) values of the normalized magnetization of ML composed of Fe_3O_4/Na ol. + H_2O]. M_s the saturation magnetization of nanoparticles in SiO_2 matrix. On *inserts* initial fragments of curves

$$\sigma_s = a - \frac{b}{1 + e^{\left(\frac{d}{c} - 2,1\right)}}, \tag{3}$$

where constants *a*, *b*, and *c* are 82.0, 92.2 Gs g^{-1} cm^3, and 3 nm, respectively. σ_s decrease with decreasing *d* may be due to the increasing role of surface spin subsystem, which does not contribute to the total magnetization of the particle.

The characteristic time of thermal fluctuations (τ_N) of magnetic moment of one-domain particle with uniaxial anisotropy on condition $KV/k_BT \geq 1$ was determined by Neel's formula [24]:

$$\tau_N = \tau_0 \exp(KV/k_BT), \tag{4}$$

where $\tau_0 = \text{const} = 10^{-9}–10^{-13}$ s, *K* is the density of energy of magnetic anisotropy, *V* is the volume of a particle, k_B is the Boltzmann constant, and *T* is the temperature. Value of τ_N increases quickly with increase in volume of a particle. For example, at $\tau_0 = 10^{-9}$ s, $K = 1.4 \times 10^5$ erg/cm^3 (the value for magnetite [27]) and $T = 300$ K, τ_N is 4.4×10^{-9}, 2.0×10^{-3}, and 10.0 s for spherical particles with diameters 9.4; 20.0, and 23.4 nm, respectively.

The blocking temperature (T_b) is defined by the condition $t_{meas} = \tau_N$, where t_{meas} is the time of magnetic characteristics measurement. At $t_{meas} = 100$ s, $\tau_0 = 10^{-9}$ s, one can obtain from a formula (4): $KV/k_BT \approx 25.3$. Then, $T_b \approx KV/25.3k_B$. The blocking temperature for the studied ensemble of particles ($d_0 = 9.38$ nm) was 135–150 K at magnetizing field of 100 Oe. Magnetite particles ($K = 1.70 \times 10^5$ erg/cm^3 [28]) with $d > 22.7$ nm come into the blocked condition at ~ 300 K and cause hysteresis (Fig. 1b).

The obtained data are in agreement with results of studies on a superparamagnetic limit (d_{crit}) for magnetite particles ($d_{crit} = 23$ nm) at 300 K [29]. Equilibrium magnetization of such ensembles is reached by the Neel mechanism of relaxation of magnetic moments of particles (4). To obtain ratios describing ensemble of identical one-domain superparamagnetic particles, the classical P. Langeven's law is used that has been deduced for magnetization of ensemble of molecules of paramagnetic gas [27]:

$$\frac{\overline{m}}{m} = cth\alpha - \alpha^{-1} \equiv L(\alpha),$$

where $\overline{m}$ is a component of an average magnetic moment of a particle along the direction of field with strength *H*, *m* is an absolute value of magnetic moment of a particle, and $L(\alpha)$ is Langeven's function, $\alpha = mH/(k_BT)$.

For a monodispersive colloidal magnetic liquid (ML):

$$\frac{\overline{m}}{m} = \frac{M(H)}{\varphi M_d} = \frac{M(H)}{M_s} = L(\alpha), \quad \alpha = \frac{\pi}{6}\frac{M_dHd^3}{k_BT}$$

where $M(H)$ is the magnetization of ML in field *H*, M_d and M_s are the saturation magnetization of a magnetic solid and magnetic liquid, respectively, and φ is the volume part of solid fraction.

For a polydispersive colloidal ML based on magnetite, it was shown [27] that matching of the experimental magnetization curve with theoretical one could be possible on assumption that Fe_3O_4 particles contained a low-magnetic

layer with thickness $d_s/2 = 0.83$ nm (the constant of magnetite lattice at 300 K is 0.824 nm). Emergence of the said layer was considered as a result of chemical interaction of a particle with a stabilizing surface active substance [30].

Thus, for a polydispersive colloidal ML [29]:

$$\frac{M(H)}{\varphi M_d} = \frac{\sum_i n_i(d_i - d_s)^3 L\left(\frac{M_d H}{k_B T}\frac{\pi}{6}(d_i - d_s)^3\right)}{\sum_i n_i d_i^3},$$
$$M(H) = n\overline{m}, M_s = nm \tag{5}$$

where d_i is an external diameter of a particle, d_i–d_s is the diameter of a magnetic nucleus, n and n_i are quantity of all particles and particles of i-th diameter in unit volume of ML, respectively; $M_d = \rho_{Fe3O4} \cdot \sigma_{sFe3O4} \approx 5.24$ g cm^{-3} × 92.0 Gs g^{-1} cm^3 ≈ 482.1 Gs.

However, measurements of Mossbauer spectra of the colloid particles of Fe_3O_4 did not show existence of a similar layer [31].

We reached matching of the said curves not by introduction of d_s parameter of a low-magnetic layer in formula (5), but by supposing that M_d depends on diameter of a particle: $M_d = \rho_{Fe3O4}\sigma_s$, where σ_s value was calculated by formula (3).

Then,

$$\frac{M(H)}{M_s} = \frac{\sum_{k=1}^{11} m_k d_k^3 \sigma_s(d_k) L\left(\frac{\rho\sigma_s(d_k)H}{k_B T}\frac{\pi}{6}d_k^3\right)}{\sum_{k=1}^{11} m_k d_k^3 \sigma_s(d_k)}, \tag{5'}$$

where m_k was computed by formula (1). Dependence of saturation magnetization of nanoparticles on their sizes was studied in [32].

The magnetic hysteresis curve for ensemble of Fe_3O_4 nanoparticles with the surface modified with sodium oleate (Na ol.) is given in Fig. 1b. The said modifying has been carried out with the purpose to prevent aggregation of magnetite nanoparticles and, according to experiment, practically does not influence the magnetization of separate particles.

Figure 1c shows the field dependences for the experimental (1) and calculated (2) by formula (5′) values of the normalized magnetization of ML composed of Fe_3O_4/Na ol. + H_2O. It is clear that the experimental and calculated results match satisfactorily. In magnetic liquids, nanoparticles carry out onward and rotary Brownian motion. Equilibrium magnetization of ML in a magnetic field can be reached by rotation of particles relative to the dispersion medium. Such mechanism of relaxation of magnetization is characterized by Brownian time of rotational diffusion τ_B that is defined by particle volume, viscosity of the medium η, and temperature. For ML on water basis ($\eta = 0.07$ g s^{-1} cm^{-1}), which contains spherical particles with sizes $d = 6$ and 34 nm, τ_B are 10^{-6} and 10^{-4} s,

respectively. At $t_{meas} = 10$ s, equilibrium magnetization of ML has time to set and $\sigma(H)$ is characterized by considerably smaller hysteresis (Fig. 1c).

Thus, it has been shown that in terms of experimentally measured distributions of nanoparticles in ensemble one can calculate a magnetization curve of magnetic liquid on their basis.

Existence of layers of DMSA, HA, APS, and PAA on magnetite surface practically did not influence magnetic properties of initial magnetite (a nanocomposite core) as well as liquids containing nanocomposites, physiological solution, and sodium oleate.

By studying IR spectra of magnetite surface (Fig. 2a, curve 1), we showed existence of the functional groups OH$^-$ with concentration of 2.2 mmol/g, or 24 μmol/m^2, at $S_{sp} = 90$ m^2/g (it was calculated in terms of thermogravimetric analysis) [5].

DMSA is attached to a surface of iron oxide by bonding of carboxyl and hydroxyl groups according to the reaction:

$$Fe_3O_4(surf) - (OH)_2 + HOOC - (CHSH)_2 - COOH$$
$$\rightarrow Fe_3O_4(surf) - (OOC)_2 - (CHSH)_2 + 2H_2O.$$
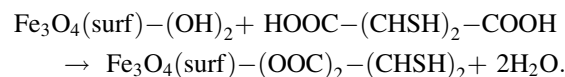
Existence of DMSA and formation of cover on a surface of magnetite were confirmed by FT-IR spectrometry (Fourier spectrometer "Perkin Elmer", 1720X model) in the range of 400–4000 cm^{-1} and X-ray photoelectron spectroscopy (electron spectrometer ES-2402 with PHOI-BOS-100-SPECS energy analyzer).

The prepared sols with DMSA-capped Fe_3O_4 nanoparticles were stable at wide pH range (3–11)—no aggregation was observed in aqueous and phosphate buffer systems.

Magnetite as well as Fe_3O_4/DMSA, Fe_3O_4/γ-APS, Fe_3O_4/PAA, and Fe_3O_4/HA nanocomposites was studied by means of IR spectroscopy. In IR spectra of Fe_3O_4/DMSA nanocomposite (Fig. 2a), three basic groups of bands at ∼550, ∼1400, ∼1630; 2505; and 2510 cm^{-1} are observed corresponding to S–S, C=O, and S–H bonds of DMSA cover on a surface of magnetite.

It has been shown by the titration method (after Kimball, Kramer, and Reid), based on the reaction: $2RSH + I_2 \rightarrow RSSR + 2HI$, that the quantity of SH groups in Fe_3O_4/DMSA nanocomposites is 2.4 mmol/g (19 μmol/m^2) at S_{sp} of magnetite of 130 m^2/g.

In IR spectra of Fe_3O_4/γ-APS nanocomposites (Fig. 2b), the absorption bands (AB) at 1052 and 1108 cm^{-1} have been registered that are characteristic for formation of polymeric structure Si–O–Si.

As a result of magnetite modification with γ-aminopropyltriethoxysilane, the surface gains alkali properties due to grafting of γ-aminopropyl groups. Concentration of reactive amino groups in the modified magnetite samples

Fig. 2 FT-IR spectra:
a magnetite (*1*), DMSA (*2*), nanocomposites Fe$_3$O$_4$/DMSA (*3*); **b** Fe$_3$O$_4$/γ-APS; **c** Fe$_3$O$_4$/PAA; **d** hydroxyapatite (*1*), nanocomposite Fe$_3$O$_4$/HA (*2*)
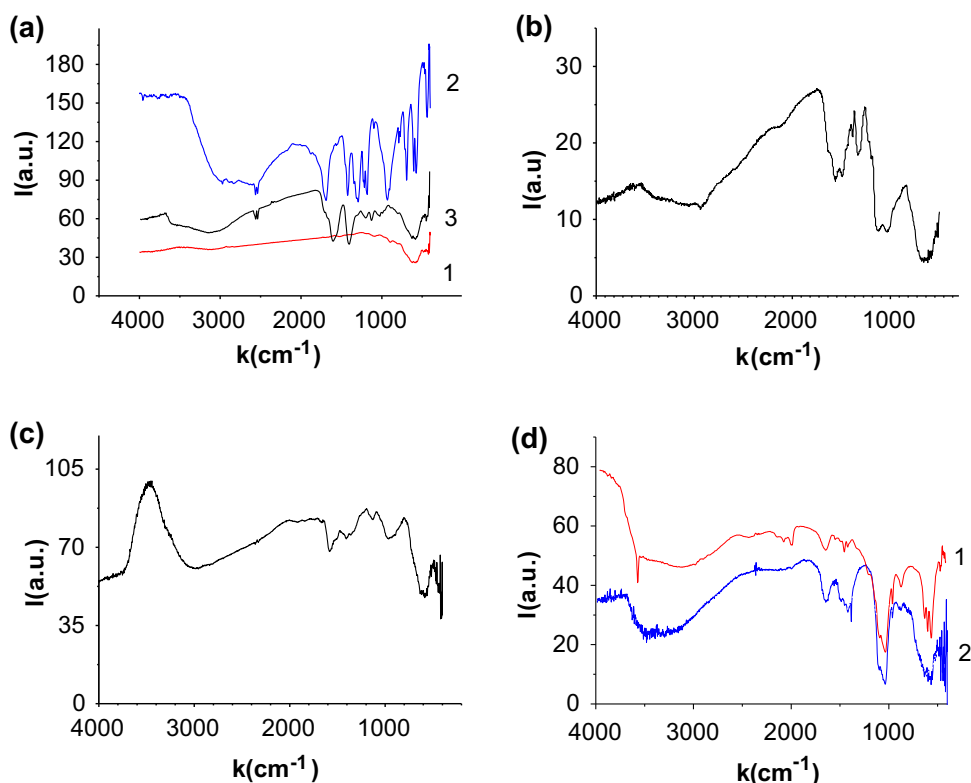
was determined using the data from thermogravimetric analysis. It was 2.2 mmol/g, or 24 μmol/m^2, at $S_{sp} = 90$ m^2/g which is in accordance with the corresponding values for concentration of OH groups for the initial magnetite.

In IR spectrum of Fe$_3$O$_4$/PAA nanocomposites (Fig. 2c), the bands are observed corresponding to vibrations of groups of the polymeric cover. Diffuse AB (maximum in the area of 2989 cm^{-1}) is due to overlapping of several bands, caused by valence vibrations of CH, CH$_2$, and NH$_2$ groups of polyacrylamide. Intensive AB at 1585 cm^{-1} is referred to valence vibrations of amide group C=O; on the side of low frequencies, the wing of this band at 1521 cm^{-1} can be attributed to deformation vibrations of NH$_2$ groups. AB at 1407 and 1359 cm^{-1} characterize the symmetric and antisymmetric deformation vibrations of CH$_2$ groups, and also deformation vibrations of CH groups. AB at 1130 cm^{-1} is referred to C–N deformation vibrations of amide group. Small intensity AB in the area of 980–560 cm^{-1} can be associated with iron oxides forming on a surface of magnetic particles under the given method of formation of PAA layer.

Analysis of IR spectra of Fe$_3$O$_4$/HA samples (Fig. 2d) shows that the wide absorption band in the area of 3500 cm^{-1} corresponds to valence vibrations of OH groups of a nanocomposite surface. AB in the area of 1380 cm^{-1}, which is absent in magnetite spectrum, corresponds to valence vibrations of P–O bonds. AB at 1645 cm^{-1} characterizes deformation vibrations of water molecules adsorbed on a nanocomposite surface. AB at 1460 cm^{-1} refers to deformation vibrations of OH groups, and also shows the presence of CO$_3^{2-}$ groups in the sample's structure. AB in the area of 1095–1100 cm^{-1} belongs to vibrations of HPO$_4^{2-}$ and PO$_4^{3-}$ groups in a structure of hydroxyapatite. AB in the area of 800–500 cm^{-1} refers to deformation vibrations of Fe–OH groups of magnetite. At heat treatment, destruction of hydrogen bonds and removal of physically bound water occur; however, due to high thermal stability of bond between OH groups and HA cation, the intensity of AB, corresponding to this group, is not decreased.

The X-ray phase analysis of magnetite samples encapsulated with hydroxyapatite was carried out on a diffractometer DRON-UM1 using Bragg–Brentano X-ray focusing (anode CoKα radiation $\lambda = 0.179021$ nm, Fe—the filter) in reflected beams (Fig. 3). According to the obtained data, the studied samples contained magnetite and hydroxyapatite. According to the data obtained, the investigated samples contained magnetite (Fe$_3$O$_4$, JCPDS No19-629), which correspond to the most intense reflections in the diffraction pattern and hydroxyapatite (Ca$_{10}$(PO$_4$)$_6$(OH)$_2$, JCPDS No74-0566), whose reflections are observed at angles $2\Theta = 30.2$; 33.7; 37.1; 37.6; 38.4; 39.8; 46.6; and 54.8°. The average size of crystal grains of

magnetite and hydroxyapatite was calculated from X-ray diffraction reflexes using the Scherrer formula.

Investigations of nanocomposites by means of X-ray photoelectron spectroscopy (XPS) were performed using an electron spectrometer ES-2402 with energy analyzer PHOIBOS-100, SPECS ($E_{MgK\alpha} = 1253.6$ eV, $V = 200$ V, $P = 2 \times 10^{-7}$ Pa). The spectrometer is equipped with ion gun IQE-11/35 and a source of low-energy electrons FG-15/40 to compensate the charging of the dielectric surface. To determine the Ca/P ratio, Ca2p- and P2p- spectra were studied (Fig. 4).

Split of the experimental Ca2p- and P2p- spectra into the separated components were made using the Gauss–Newton method. The area of the components was determined after deduction of non-linear background with Shirley method [33]. The obtained areas of the components in total give the value proportional to the atomic concentration of the element. To obtain the calibration spectrum, Ca2p- and P2p- spectra of standard hydroxyapatite specimen were also measured.

Ca2p- spectra of nanocomposite samples are given in Fig. 4a. The binding energy of a maximum of Ca2p$_{3/2}$-lines is 351 eV which coincides with the values for
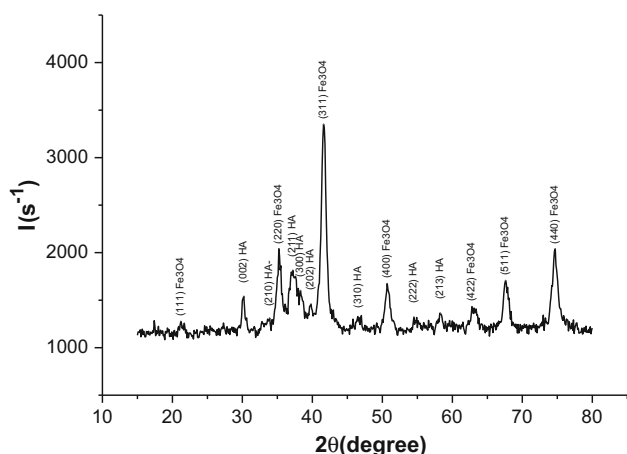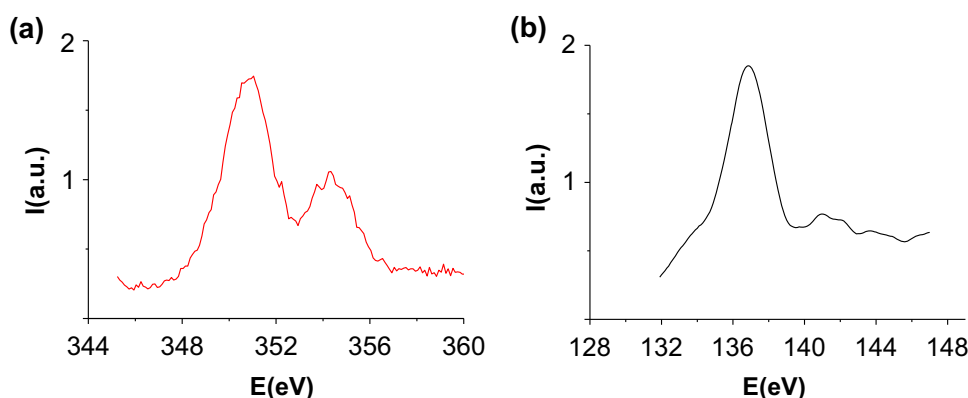
hydroxyapatite (351–352 eV). The binding energy of a maximum of P2p- line is 137 eV (Fig. 4b) which also coincides with the values for hydroxyapatite (137–138 eV) [34].

According to the XPS data, for the synthesized nanocomposites the ratio Ca/P was changed within the interval 1.6–1.7. This is close to the optimal stoichiometric value for hydroxyapatite (Ca/P = 1.67). Thickness of hydroxyapatite layer on a surface of magnetite nanoparticles, determined by a ratio of the areas of Fe2p-/Fe3p-lines and by an increase in mass of a nanocomposite, was ∼4 nm.

The samples of magnetite and nanocomposites with surfaces of various chemical nature (Fe_3O_4/DMSA, Fe_3O_4/γ-APS, Fe_3O_4/PAA, Fe_3O_4/HA) were used for studies on adsorption of *cis*-dichlorodiammineplatinum complexes.

The obtained results showed dependence of adsorption capacity of a surface of the studied samples on the chemical nature of their surface. Experimental data show that increase in equilibrium concentration of *cis*-dichlorodiammineplatinum leads to the adsorption saturation of adsorbents. Such form of isotherms can be described by Langmuir equation which is applicable for adsorbents with energetically equivalent adsorption centers.

First of all, one should note the considerable adsorption activity of nanosized magnetite with respect to *cis*-dichlorodiammineplatinum complexes. Thus, at 298 K for Fe_3O_4 $A = 80.1$ mg/g, $R = 66.2$ % (Fig. 5a, b, curves 1).

Emergence of thiol functional groups on Fe_3O_4 surface, due to modification with DMSA, increases adsorption capacity. For Fe_3O_4/DMSA nanocomposites $A = 83.4$ mg/g (Fig. 5a, curve 2), extraction extent reaches 85.40 % (Fig. 5b, curve 2). Studies on adsorption kinetics show that the main quantity of *cis*-dichlorodiammineplatinum is adsorbed on Fe_3O_4/DMSA in 10 – 20 min (Fig. 5b, curve 2).

Formation of the active NH$_2$-groups on a surface of Fe_3O_4 as a result of its modification with γ-APTES also leads to an increase in adsorption capacity of magnetosensitive nanocomposites (Fig. 5a, curve 3). A value derived from the corresponding adsorption isotherm for

Fig. 3 X-ray diffractogram of Fe_3O_4/HA nanocomposite

Fig. 4 X-ray photoelectron Ca2p- (**a**) and P2p- (**b**) spectra of Fe_3O_4/HA nanocomposite

Fe₃O₄/γ-APS composite at 298 K is 84.0 mg/g at extraction extent of 93.8 % (Fig. 5b, curve 3). For this composite, equilibrium sets faster—the main quantity of Pt^{2+} complexes is adsorbed on Fe₃O₄/γ-APS in 10 min.

Still larger values of adsorption of *cis*-dichlorodiammineplatinum were observed for a surface of Fe₃O₄/PAA nanocomposites (Fig. 5a, curve 4). *A* value derived from the corresponding adsorption isotherm for Fe₃O₄/PAA nanocomposite was 109.5 mg/g at extraction extent of 99.9 % (Fig. 5b, curve 4).

Magnetite modification with hydroxyapatite, unlike DMSA, γ-APTES and PAA, reduces the adsorption activity with respect to *cis*-dichlorodiammineplatinum (Fig. 5a, curve 5): *A* = 54.0 mg/g, extraction extent *R* = 64.8 % (Fig. 5b, curve 5). Probably, this occurs due to a decrease in quantity of hydroxyl groups on a surface of Fe₃O₄/HA nanocomposite in comparison with a surface of initial magnetite. Time of setting equilibrium for a surface of Fe₃O₄/HA nanocomposite (Fig. 5b, curve 5) remains within the limits similar for the studied composites—10 min.

Table 1 shows the adsorption capacities for the studied nanostructures *A*, mg/g (with respect to Pt^{2+} ions), the calculated values of distribution coefficient (*E*, L/g), and the extraction extent of *cis*-dichlorodiammineplatinum (*R* %) at the maximum concentration of initial solution $C_0 = 200$ mg/L and a weight of 0.1 g.

It can be seen that the adsorption parameters depend on the chemical nature of a surface. Thus, after modification of magnetite with DMSA, APTES, and PAA the distribution coefficients considerably exceed the corresponding value for initial Fe₃O₄ which shows equilibrium displacement towards immobilization of a substance on a surface. The latter confirms the active participation of functional thiol and amino groups in adsorption processes of *cis*-dichlorodiammineplatinum. However, after modification of a magnetite surface with hydroxyapatite, *E* value decreases almost twice in comparison with native Fe₃O₄ surface (Table 1).

The best adsorption parameters were obtained for Fe₃O₄/PAA and Fe₃O₄/γ-APS nanocomposites. This can be explained by the ability of amino groups to form complexes with platinum ions [35].

The greatest adsorption is found for Fe₃O₄/PAA nanocomposites which can be caused by developed structure of polyacrylamide cover, typical for the used method of polymerization.

Mechanisms of adsorption of platinum complexes on a surface of the synthesized nanostructures will be specified by us later; however, we notice that existence of hydroxyl or thiol groups on a surface of nanostructures can cause ion exchange and complexation, respectively [35]. The composite nature of formation of chelate complexes of dimercapto-chelating agents with metals or metalloids should be also taken into account [19]. Thus, for example, it has been shown by experiments with the use of NMR and IR spectrometry in combination with potentiometric titration of DMSA suspensions that Pb^{2+} or Cd^{2+} ions are coordinated

Fig. 5 Isotherms (**a**) and extraction degree vs contact time (**b**) of *cis*-dichlorodiammineplatinum adsorption on magnetite (*1*), nanocomposites Fe₃O₄/DMSA (*2*), Fe₃O₄/γ-APS (*3*), Fe₃O₄/PAA (*4*), Fe₃O₄/HA (*5*)
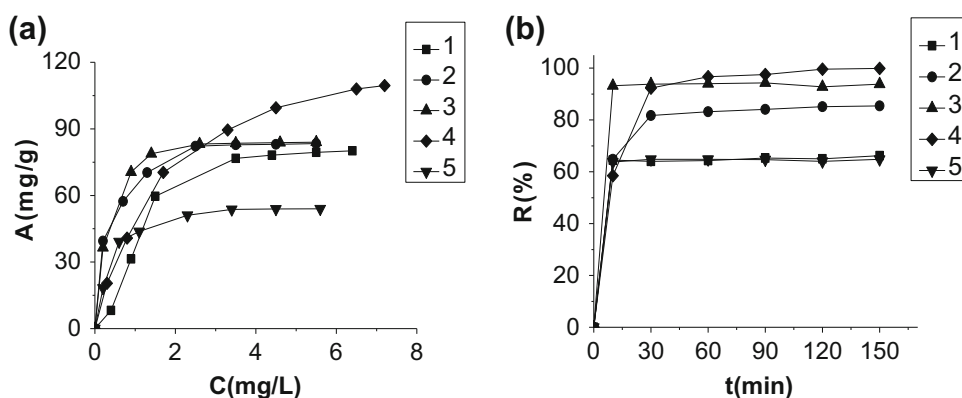
Table 1 Adsorption of *cis*-dichlorodiammineplatinum by nanostructures with various chemical nature of a surface

Type of nanostructure	Adsorption capacity *A*, mg/g	Distribution coefficient *E*, L/g	Extraction extent *R*, %
Fe₃O₄	80.10	2.16	66.20
Fe₃O₄/DMSA	83.40	4.77	85.40
Fe₃O₄/γ-APS	84.00	12.92	93.80
Fe₃O₄/PAA	109.50	16.20	99.90
Fe₃O₄/HA	54.00	1.08	64.80

with one atom of sulfur and one atom of oxygen of DMSA. On the other hand, Hg^{2+} or Ni^{2+} is coordinated with each of two atoms of sulfur. Thus, the nature of coordinating with participation of DMSA depends on metal ion type.

It should be noted that in recent years in the literature there is considerable interest to development of magnetic adsorbents, in particular, based on magnetite, as well as to the study of their properties and modeling processes occurring on the surface. Thus, adsorption by magnetosensitive nanocomposites and by modified surfaces of different chemical nature has been studied with respect to heavy metal ions [36–39], organic and biological molecules [40–43], and anti-cancer drugs [44–46]. Clarification of mechanisms and theoretical modeling of platinum complexes adsorption on the surface of synthesized nanostructures with considering of the surface state, the nature of the surface active centers and their concentration, will be performed by us later.

In vitro and in vivo studies of nanoscale magnetite modified with DMSA, γ-APTES, PAA, and HA [5, 10] confirmed its high biocompatibility, absence of mutagenicity, and the possibility of practical use of the nanocomposites in biomedical purposes. On their basis, the prototypes of magnetically operated drugs containing cytotoxic drug cisplatin (active ingredient—*cis*-dichlorodiammineplatinum) were produced for cancer tests.

The optimum magnetic properties and adsorption parameters of investigated in this work nanocomposites Fe_3O_4/DMSA, Fe_3O_4/γ-APS, Fe_3O_4/PAA, Fe_3O_4/HA with respect to *cis*-dichlorodiammineplatinum, as well as the possibility of using in liquid media, including biological, indicate the prospects for their use as adsorbents of *cis*-dichlorodiammineplatinum for biomedical (detoxification) and technical (platinum recycling solutions) purposes. Particular interest in this context can be provided with magnetic quantum dots with properties of artificial atoms [47, 48], which may have not only promising adsorption parameters but also fulfill functions of directional transport of *cis*-dichlorodiammineplatinum in local oncotherapy, intracellular optical sensors, etc.

Conclusions

The single-domain magnetite and magnetosensitive nanocomposites Fe_3O_4/DMSA, Fe_3O_4/γ-APS, Fe_3O_4/PAA, Fe_3O_4/HA were synthesized. The size distribution of magnetite nanoparticles in ensemble and their magnetic properties were studied. The calculations of magnetization curve for magnetic liquid based on single-domain Fe_3O_4 in the framework of Langeven's paramagnetism theory match satisfactorily to the experimental results in assumption that saturation magnetization of magnetite particles depends on their sizes.

The isotherms and kinetics of adsorption of *cis*-dichlorodiammineplatinum were studied depending on chemical nature of a surface of nanostructures. Prospects of use of the studied nanostructures for elaboration of adsorbents of *cis*-dichlorodiammineplatinum for medico-biological and technical purpose were shown. The highest adsorption parameters were demonstrated for magnetosensitive nanocomposites Fe_3O_4/PAA and Fe_3O_4/γ-APS.

References

1. Greg, S., Sing, K.: Adsorbtsiya, udelnaya poverkhnost', poristost'. Mir, Moskva. http://www.twirpx.com/file/100985/ (1984)
2. Zagrebin, L.V., Shestov, S.S., Yanovskiy, Y.G., Danilin, A.N., Zhogin, V.A., Alyochin, A.I., Goncharov, N.N.: Metod ochistki krovi ot virusnoy infektsii putyom sorbtsii na magnitoupravlyayemykh nanochastitsakh. Tekhnologii zhyvykh sistem. **5**(2–3) 111. http://istina.msu.ru/publications/article/7061391/ (2008)
3. Yanovskiy, Y.G., Danilin, A.N., Zakharov, A.P., Zhogin, V.A.: Opytno-konstruktorskiye razrabotki portativnogo ustroystva dlya ekstrakorporalnoy ochistki biologicheskikh sred organizma ot toksinov i virusov s ispolzovaniyem magnitochuvstvitelnykh nano- i mikrochastits. Almanakh klinicheskoy medizyny. III Troitskaya konferentsiya "Meditsynskaya fizika i innovatsii v meditsyne". Moskva. **17**(2), 293 (2008)
4. Nanomaterials and supramolecular structures. Physics Chemistry and Applications. In: Shpak, A.P., Gorbyk, P.P. (eds.) Springer. http://www.springer.com/cn/book/9789048123087 (2009)
5. Gorbyk, P.P., Turov, V.V.: Nanomaterialy i nanokompozity v medizyne, biologii, ekologii. In: Shpak, A.P., Chekhun, V.F. (eds.). Naukova dumka, Kiev. http://www.irbis-nbuv.gov.ua/ (2011)
6. Gorbyk, P.P., Gorobez', S.V., Turelyk, M.P., Chekhun, V.F., Shpak, A.P.: Biofunktsionalizatsiya nanomaterialiv i nanokompozytiv. Naukova dumka, Kyiv. http://www.irbis-nbuv.gov.ua/ (2011)
7. Mishchenko, V.M., Kartel', M.T., Lutsenko, V.A., Nikolaichuk, A.D., Kusyak, N.V., Korduban, O.M., Gorbyk, P.P.: Magnitochutlyvi adsorbenty na osnovi aktyvovanogo vugil'ya: syntez ta vlastyvosti. Poverkhnost'. Mizhvid. zb. nauk. prats'. Kyiv. **2**(17), 276. http://dspace.nbuv.gov.ua/bitstream/handle/123456789/39341/26-Mishchenko.pdf?sequence=1 (2010)

8. Kolotilov, S.V., Boltovets, P.N., Snopok, B.A., Pavlishchuk, V.V.: Nanorazmernyi magnitnyi kompozit dlya izvlecheniya γ-immunoglobulinov iz biologicheskikh sred. Teoreticheskaya i eksperimentalnaya khimiya. **42**(4), 204. http://www.inphyschem nas.kiev.ua/ua/magazine/archive/journals/2006/annotations4/2 (2006)

9. Semko, L.S., Khutornyi, S.V., Storozhuk, L.P., Dzyubenko, L.S., Abramov, N.V., Gorbyk, P.P.: Khimichne konstruyuvannya ta doslidzhennya vlastyvostey magnitokerovanykh adsorbentiv dlya ekstraktsiyi nukleyinovykh kyslot. Poverkhnost'. Mizhvid. zb. nauk. prats'. Ќyiv. **2**(17), 330 http://dspace.nbuv.gov.ua/bitstream/handle/123456789/39345/30-Semko.pdf?sequence=1 (2010)

10. Gorbyk, P.P., Chekhun, V.F.: Nanocomposites of medicobiologic destination: reality and perspectives for oncology. Funct. Mater. **19**(2), 145 http://functmaterials.org.ua/contents/19-2/fm192-01.pdf (2012)

11. Turanska, S.P., Kaminskyi, A.N., Kusyak, N.V., Turov, V.V., Gorbyk, P.P.: Sintez, svoystva i primeneniye magnitoupravlyayemykh adsorbentov. Poverkhnost'. Mizhvid. zb. nauk. prats'. Ќyiv. **4**(19), 266. http://surfacezbir.com.ua/images/Arhiv/N19/3/3-9Turanska266-292.pdf (2012)

12. Astashkina, O.V., Mikhalchan, А.А., Simanova, S.A., Lysenko, А.А.: Adsorbtsiya ionov platiny, palladiya i zolota uglerodnymi nanotrubkami, tekhnicheskim uglerodom i aktivirovannym uglyom. Izvestiya vysshykh uchebnykh zavedeniy. Tekhnologiya lyogkoy promyshlennosti. **17**(3), 40 http://journal.prouniver.ru/tlp/tlp-archive1/3-2012-e/#eng (2012)

13. Oborotova, N.A.: Napravlennaya dostavka protivoopukholevykh preparatov. Antibiotiki i khimioterapiya. **36**(10), 47 (1991)

14. Kris, Ё.Е., Volchenskova, I.I., Grigoryeva, A.S., Yatsimirskyi, K.B., Budarin, L.I.: Koordinatsionnyye soyedineniya metallov v meditsyne. Naukova dumka, Kiev (1986)

15. Kusyak, N.V., Kaminskyi, O.M., Petranovska, A.L., Gorbyk, P.P.: Adsorbtsiya kationov na poverkhnosti nanorazmernogo magnetita. Poverkhnost'. Mizhvid. zb. nauk. prats'. Ќyiv. **3**(18), 151. http://surfacezbir.com.ua/images/Arhiv/N18/2/27.pdf (2011)

16. Guan, B., Zou, F., Zhi, J.: Nanodiamond as the pH-Responsive vehicle for an anticancer drug. Small. **6**(14), 1514–1519 http://onlinelibrary.wiley.com/doi/10.1002/smll.200902305/abstract (2010)

17. Múzquiz-Ramos, E.M., Guerrero-Chávez, V., Macías-Martínez, B.I., López-Badillo, C.M., García-Cerda, L.A.: Synthesis and characterization of maghemite nanoparticles for hyperthermia applications. Ceramics. Int. **41**(1), 397–402. http://www.sciencedirect.com/science/article/pii/S0272884214013200 (2015)

18. Aposhian, H., Aposhian M.: Meso-2,3-dimercaptosuccinic acid: chemical, pharmacological and toxicological properties of an orally effective metal chelating agent. Annu. Rev. Pharmacol. Toxicol. **30**, 279. http://onlinelibrary.wiley.com/doi/10.1002/smll.200902305/abstract (1990)

19. Yantasee, W., Warner, C.L., Sangvanich, T., Addleman, R.S., Carter, T.G., Wiacek, R.J., Fryxell, G.E., Timchalk, C., Warner, M.G.: Removal of heavy metals from aqueous systems with thiol functionalized superparamagnetic nanoparticles. Environ. Sci. Technol. **41**(14), 5114. http://pubs.acs.org/doi/abs/10.1021/es0705238 (2007)

20. Petranovska, A.L., Fedorenko, О.М., Storozhuk, L.P., Gorbyk, P.P., Chuiko, А.А., Dzyubenko, L.S., Oranska, Ye.I.: Modifitsyrovaniye nanochastits magnetita γ-aminopropiltrietoksisilanom zhydkofaznym metodom. Doklady NAN Ukrainy. **1**, 157 (2006)

21. Borisenko, N.V., Bogatyrev, V.M., Dubrovin, I.V., Abramov, N.V., Gayeva, M.V., Gorbyk, P.P.: Sintez i svoystva magnitochuvstvitelnykh nanokompozitov na osnove oksidov zheleza i kremniya. Fiziko-khimiya nanomaterialov i supramolekulyarnykh struktur. Shpak, A.P., Gorbyk, P.P. (eds.). Naukova dumka, Ќiev **1**, 394. http://www.irbis-nbuv.gov.ua/cgi-bin/irbis_nbuv/ (2007)

22. Turov, V.V., Gorbyk, S.P.: Opredeleniye sil adgezii na mezhfaznoy granitse kletka/voda iz dannykh ¹Ḣ YaMR spektroskopii. Ukrainskiy khimicheskiy zhurnal **69**(6), 80 (2003)

23. Turov, V.V., Gorbyk, S.P., Chuiko, А.А.: Vliyaniye dispersnogo kremnezema na svyazannuyu vodu v zamorozhennykh kletochnykh suspenziyakh. Problemy kriobiologii **3**, 16 (2002)

24. Ivanova, V.M., Kalinina, V.N., Neshumova, L.A., Reshetnikova, I.O.: Matematicheskaya statistika. Vysshaya shkola, Moskva (1975)

25. Abramov, N.V., Gorbyk, P.P.: Svoystva ansambley nanochastits magnetita i magnitnykh zhydkostey dlya primeneniy v onkoterapii. Poverkhnost'. Mizhvid. zb. nauk. prats'. Ќyiv. **4**(19), 246. http://surfacezbir.com.ua/images/Arhiv/N19/3/3-8Abramov246-265.pdf (2012)

26. Neel, L.: Influence of thermal fluctuations on the magnetization of ferromagnetic small particles. C. R. Acad. Sci. **228**(6), 664 (1949)

27. Rozentsveyg, R.: Ferrogidrodinamika. Mir, Moskva. http://www.twirpx.com/file/179455/ (1989)

28. Shtrikman, S., Wohlfarth, E.P.: The theory of the Vogel–Fulcher law of spin glasses. Phys. Lett. A. **85**(8–9), 467 (1981)

29. Kim, T., Reis, L., Rajan, K., Shima, M.: Magnetic behavior of iron oxide nanoparticle–biomolecule assembly. J. Magn Magn Mater **295**, 132. http://www.sciencedirect.com/science/journal/03048853/295/2 (2005)

30. Shliomis, M.I.: Magnitnyye zhydkosti. UFN **112**(3), 427 (1974)

31. Fertman, V.Y.: Magnitnyye zhydkosti. Vysshaya shkola. Minsk (1988)

32. Kim, T., Shima, M.: Reduced magnetization in magnetic oxide nanoparticles. J. Appl. Phys. **101**, 09M516. http://connection.ebscohost.com/c/articles/25114951/reduced-magnetization-magnetic-oxide-nanoparticles (2007)

33. Nefedov, V.I.: Rentgenoelektronnaya spektroskopya hymycheskyh soedineniy. Khimia, Moskva (1984)

34. Wagner, C.D., Moulder, J.F., Davis, L.E., Riggs, W.M.: Handbook of X-ray Photoelectron Spectroscopy. Perking-Elmer Corp, New York (1979)

35. Khimiya poverkhnosti kremnezema. Chuiko, А.А. (ed.) Kiev **1**(1), 736. http://www.irbis-nbuv.gov.ua/ (2001)

36. Goon, I.Y., Zhang, C., Lim, M., Gooding, J.J., Amal, R.: Controlled fabrication of polyethylenimine-functionalized magnetic nanoparticles for the sequestration and quantification of free Cu^{2+}. Langmuir. **26**(14) 12247–12252 http://pubs.acs.org/doi/abs/10.1021/la101196r (2010)

37. Liang, B.: Adsorption characteristics of Hg^{2+} ions using Fe_3O_4/chitosan magnetic nanoparticles. Adv. Mater. Res. **291–294**, 72–75. http://www.scientific.net/AMR.291-294.72 (2011)

38. Wang, J., Zheng, S., Shao, Y., Liu, J., Xu, Z., Zhu, D.: Aminofunctionalized Fe_3O_4/SiO_2 core-shell magnetic nanomaterial as a novel adsorbent for aqueous heavy metals removal. J.Colloid. Interface. Sci. **349**(1) 293–299. http://www.sciencedirect.com/science/article/pii/S0021979710005199 (2010)

39. Park, M., Seo, S., Lee, I.S., Jung, J.H.: Ultraefficient separation and sensing of mercury and methylmercury ions in drinking water by using aminonaphthalimide-functionalized Fe_3O_4/SiO_2 core/shell magnetic nanoparticles. Chem. Commun. **46**(25), 4478–4480. http://pubs.rsc.org/en/Content/ArticleLanding/2010/CC/C002905J#!divAbstract (2010)

40. Weng, C.-H., Lin, Y.-T., Yeh, C.-L., Sharma, Y.C. Magnetic Fe_3O_4 nanoparticles for adsorptive removal of acid dye (new coccine) from aqueous solutions. Water. Sci. Technol. **62**(4), 844–851. http://europepmc.org/abstract/MED/20729587 (2010)

41. Yu, C.-J., Lin, C.-Y., Liu, C.-H., Cheng, T.-L., Tseng, W.-L.: Synthesis of poly(diallyldimethylammonium chloride)-coated Fe_3O_4 nanoparticles for colorimetric sensing of glucose and selective extraction of thiol. Biosens. Bioelectron. **26**(2), 913–917 http://www.ncbi.nlm.nih.gov/pubmed/20656467 (2010)

42. Thio, B.J., Clark, K.K., Keller, A.A.: Magnetic pollen grains as sorbents for facile removal of organic pollutants in aqueous media. J. Hazard. Mater. **194**, 53–61. http://www.sciencedirect.com/science/article/pii/S0304389411009514 (2011)

43. Qiu, J.D., Peng, H.P., Liang, R.P., Xia, X.H.: Facile preparation of magnetic core-shell Fe_3O_4/Au nanoparticle/myoglobin biofilm for direct electrochemistry. Biosens. Bioelectron. **25**(6), 1447–1453. http://www.sciencedirect.com/science/article/pii/S09565663090060 22 (2010)

44. Gu, L., Park, J.H., Duong, K.H., Ruoslahti, E., Sailor, M.J.: Magnetic luminescent porous silicon microparticles for localized delivery of molecular drug payloads. Small. **6**(22), 2546–2552. http://www.ncbi.nlm.nih.gov/pmc/articles/PMC3033739/ (2010)

45. Ma, Y., Manolache, S., Denes, F., Vail, D., Thamm, D., Kurzman, I.: Plasma synthesis of carbon-iron magnetic nanoparticles and immobilization of doxorubicin for targeted drug delivery. J. Mater. Eng. Perform. **15**(3), 376–382. http://link.springer.com/article/10.1361%2F105994906X113705#page-1 (2006)

46. Zhu, A., Yuan, L., Jin, W., Dai, S., Wang, Q., Xue, Z., Qin, A.: Polysaccharide surface modified Fe_3O_4 nanoparticles for camptothecin loading and release. Acta. Biomater. **5**(5), 1489–1498. http://www.sciencedirect.com/science/journal/17427061/5/5 (2009)

47. Pokutnyi, S.I., Gorbyk, P.P.: New model superatom in nanogeterostructures. J. Nanostruct. Chem. **4**(10), 44 http://www.sciencepublishinggroup.com/journal/paperinfo.aspx?journalid= 126&doi=10.11648/j.optics.s.2014030601.15 (2014)

48. Advances in Semiconductor Research: Physics of Nanosystems, Spintronics and Technological Applications. Adorno, D.P., Pokutnyi, S. (eds.) New York: Nova Science Publishers. http://www.amazon.com/Advances-Semiconductor-Research-Technological-Applications/dp/1633217558 (2014)